Tunable unidirectional compact acoustic amplifier via space-time modulated membranes

Xiaohui Zhu,[1,2] Junfei Li,[2] Chen Shen,[2] Guangyu Zhang,[1] Steven A. Cummer,[2,*] and Longqiu Li[1,†]
[1]*State Key Laboratory of Robotics and System, Harbin Institute of Technology, Harbin, Heilongjiang 150001, China*
[2]*Department of Electrical and Computer Engineering, Duke University, Durham, North Carolina 27708, USA*

(Received 7 May 2020; revised 13 July 2020; accepted 16 July 2020; published 30 July 2020)

Space-time modulation has recently attracted considerable attention as it enables new possibilities in wave manipulation and control. Here we propose a tunable unidirectional acoustic amplifier based on a space-time modulated membrane system. The transfer matrix method is applied to design this system and optimize the modulation parameters for the realization of unidirectional amplification. Efficient one-way amplification of acoustic waves is demonstrated theoretically and numerically within a frequency range from 2260 to 2520 Hz, with overall dimension being less than $1/3$ of the corresponding wavelength. Across this operation band, the amplification factor in the positive direction varies smoothly from 3.0 to 5.8, while the transmitted wave energy in the negative direction does not change significantly. Our work identifies a feasible approach to realize a tunable unidirectional acoustic amplifier via space-time modulated membranes, which offers a design platform for a number of applications in sensing, imaging, and communication.

DOI: 10.1103/PhysRevB.102.024309

I. INTRODUCTION

Space-time modulated systems are dynamic structures whose constitutive parameters vary in both space and time. As time is introduced as an additional design degree of freedom, unusual properties can emerge that are completely different than those of conventional materials. These properties exhibit interesting physics and can also enable novel functionalities. In the 1950s and 1960s, space-time modulation was first studied in transmission lines to break the time-reversal symmetry, with one of the most studied applications being parametric amplification [1–8]. In that era, variable inductance or capacitance was the most common means of creating space-time modulated systems, which suffered from bulkiness, nonintegrability and incompatibility with high frequency techniques.

Recently, thanks to the development of newer modulation techniques, space-time modulation has been rediscovered and attracted considerable attention through introduction into modern electromagnetics and acoustics. In electromagnetics, various microwave and optical components have been realized by applying space-time modulation, such as isolators [9–15], circulators [16,17], frequency mixers [18], one-way beam splitters [19], metasurfaces [20,21], and nonreciprocal antenna [15,22–24]. Despite success in electromagnetics, only a few space-time modulated devices in acoustics have been demonstrated, although the underlying physics share a lot of similarities with those of electromagnetic waves. This is primarily due to the lack of effective modulation techniques. Nearly all the reported acoustic space-time modulated systems are based on resonators with space-time modulated cavities [25–30]. Elastic membranes, another important element in acoustic metamaterials [31] and metasurfaces [32], have yet to be explored in space-time modulation. It was shown that compared with Helmholtz resonators, a piezoelectric membrane-based space-time modulated system has several significant advantages including small insertion loss, tunable working frequency without modifying the geometric configuration, and negligible noise from modulated elements [33].

Unidirectional parametric amplification can be achieved through phase matching in space-time modulation media [28], which usually requires bulky numerous modulated elements. However, in this work, we show that this functionality can be realized using a fairly simple design, with overall dimension being less than $1/3$ of the corresponding wavelength. This compact unidirectional acoustic amplifier is composed of a waveguide and two membranes whose surface tensions are temporally modulated. Previous research has shown that the input acoustic wave will be amplified by careful selection of the modulating frequency. In addition, the phase difference between two membranes introduces a directional bias into the system, which leads to the nonreciprocity in the system. By carefully engineering these two parameters, unidirectional amplification can be realized. Furthermore, by changing the static surface tension of the membrane, the effective working frequency band can be adjusted, which means a tunable unidirectional acoustic amplifier is quite possible without altering the geometric configuration. The transfer matrix method for a one-dimensional system with serial loads is applied to analyze and optimize this membrane system [30].

II. MATHEMATICAL MODELING

We begin with the theoretical analysis of the two-membrane system, a schematic diagram of which is shown

*Corresponding author: cummer@ee.duke.edu
†Corresponding author: longqiuli@hit.edu.cn

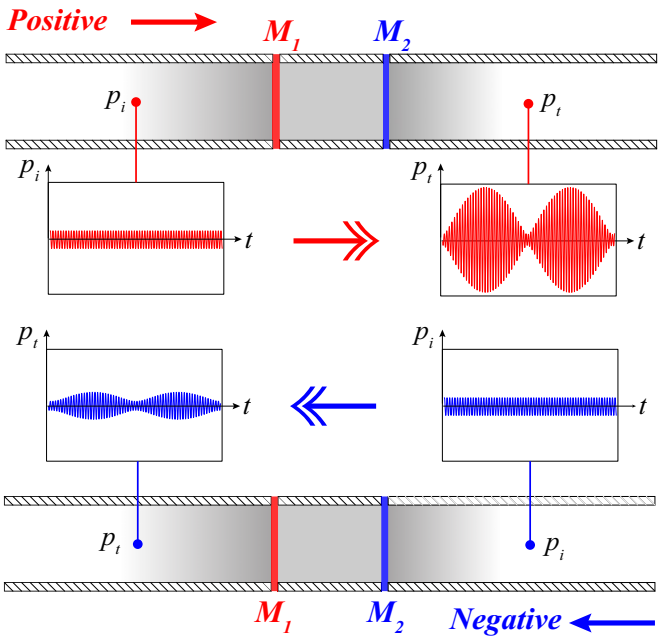

FIG. 1. Schematic diagram of the acoustic amplifier. Two temporally modulated membranes are fixed around the edge in the waveguide. p_i: monochromatic incident wave; p_t: modulated transmitted wave with high order harmonics.

in Fig. 1. The system consists of a circular tube and two membranes that are clamped in the tube. The radius of the tube and membrane is denoted as R, and the distance between two membranes is D. The tube wall is considered to be sound rigid, and the background medium is air whose density and sound speed are ρ_0 and c_0, respectively. The membrane is made of silicone rubber with thickness d, density ρ_m, Young's modulus E_m, and shear modulus G_m. Time-varying surface tensions in the form of $T_i = T_0[1 + m\cos(\Omega t - \phi_i)]^2$ $(i = 1, 2)$ are applied to these two membranes. The surface tension function here needs to be squared so as to achieve the desired sinusoidally modulated sound speed and impedance, as indicated by the equation $c_{m0} = \sqrt{\frac{T_0}{\rho_m d}}$. In practice, the required surface tension modulation can be realized by applying AC voltages on piezoelectric membranes, which shows a promising aspect in terms of feasibility [34]. Here m is the modulation depth, Ω is the modulation angular frequency, and ϕ_i is the initial phase of the modulation. Because of the modulation, when a monochromatic acoustic wave is incident into the system, the Floquet components will be generated and the transmitted wave is highly modulated as shown in the inset of Fig. 1. The frequency of the nth mode are $\omega_n = \omega_0 + n\Omega$ $(n = \ldots, -2, -1, 0, 1, 2, \ldots)$.

According to the transfer matrix method [30], this system can be divided into two types of acoustic elements (waveguide and membrane), and each of them can be represented by a transfer matrix. First, we derive the transfer matrix of the membrane. The equivalent impedance of the modulated membrane is $Z_m(\omega) = -j\omega\rho_m d[J_0(\frac{\omega R}{c_m})]/[J_2(\frac{\omega R}{c_m})]$ [35]. J_0 and J_2 are the zeroth order and second order Bessel functions of the first kind. Under weak modulation ($m \leqslant 0.1$ in this space-time modulated system) we can expand the impedance at c_{m0} as

$$Z_m(\omega) = Z_{m0}(\omega) + mZ_{v0}(\omega)\cos(\Omega t - \phi), \tag{1}$$

where $c_{m0} = \sqrt{\frac{T_0}{\rho_m d}}$ is the sound speed of the unmodulated membrane, $Z_{m0} = Z_m|_{c_m = c_{m0}}$ and $Z_{v0} = c_{m0}\frac{\partial Z_m}{\partial c_m}|_{c_m = c_{m0}}$. A plane wave is launched into the waveguide with angular frequency ω_0. Due to the time-varying impedance of the membrane, harmonics will be generated. The pressure and velocity on the upstream and downstream of the membrane can be written as

$$p_{\mp} = \sum_{n=-\infty}^{\infty} p_{\mp}^n e^{j\omega_n t}, \tag{2}$$

$$v_{\mp} = \sum_{n=-\infty}^{\infty} v_{\mp}^n e^{j\omega_n t}. \tag{3}$$

The boundary condition at the position of the membrane should satisfy

$$p_- - p_+ = \sum_{n=-\infty}^{\infty} Z_m^n v_+^n e^{j\omega_n t}, \tag{4}$$

$$v_- = v_+, \tag{5}$$

where the superscript denotes the impedance of the membrane at each order of harmonics, i.e., $Z_m^n = Z_m(\omega_n)$ and so on. Put the expression of the membrane's impedance, pressure, and velocity into Eqs. (4) and (5), equate the terms with $e^{j\omega_n t}$ using the relation $\cos(\Omega t - \phi) = \frac{1}{2}[e^{j(\Omega t - \phi)} + e^{-j(\Omega t - \phi)}]$, we can rewrite the boundary conditions in terms of each order of the harmonics:

$$p_-^n - p_+^n = Z_{m0}^n v_+^n + \frac{mZ_{v0}^{n-1}}{2} e^{-j\phi} v_+^{n-1} + \frac{mZ_{v0}^{n+1}}{2} e^{j\phi} v_+^{n+1}, \tag{6}$$

$$v_-^n = v_+^n, \tag{7}$$

where $Z_{m0}^n = Z_{m0}(\omega_n)$ and $Z_{v0}^n = Z_{v0}(\omega_n)$. The transfer matrix of the membrane M_m is defined as

$$\begin{bmatrix} \vdots \\ p_-^{n-1} \\ v_-^{n-1} \\ p_-^n \\ v_-^n \\ p_-^{n+1} \\ v_-^{n+1} \\ \vdots \end{bmatrix} = M_m \begin{bmatrix} \vdots \\ p_+^{n-1} \\ v_+^{n-1} \\ p_+^n \\ v_+^n \\ p_+^{n+1} \\ v_+^{n+1} \\ \vdots \end{bmatrix}. \tag{8}$$

With the boundary conditions, the transfer matrix of the membrane can be written as

$$M_m = \begin{bmatrix} & \vdots & \vdots & \vdots & \vdots & \vdots & \vdots & \\ \dots & 1 & Z_{m0}^{n-1} & 0 & \frac{mZ_{v0}^{n}}{2}e^{j\phi} & 0 & 0 & \dots \\ \dots & 0 & 1 & 0 & 0 & 0 & 0 & \dots \\ \dots & 0 & \frac{mZ_{v0}^{n-1}}{2}e^{-j\phi} & 1 & Z_{m0}^{n} & 0 & \frac{mZ_{v0}^{n+1}}{2}e^{j\phi} & \dots \\ \dots & 0 & 0 & 0 & 1 & 0 & 0 & \dots \\ \dots & 0 & 0 & 0 & \frac{mZ_{v0}^{n}}{2}e^{-j\phi} & 1 & Z_{m0}^{n+1} & \dots \\ \dots & 0 & 0 & 0 & 0 & 0 & 1 & \dots \\ & \vdots & \vdots & \vdots & \vdots & \vdots & \vdots & \end{bmatrix}. \tag{9}$$

And the transfer matrix of the waveguide can be written directly,

$$M_w = \begin{bmatrix} & \vdots & \vdots & \vdots & \\ \dots & M_w^{n-1} & 0 & 0 & \dots \\ \dots & 0 & M_w^{n} & 0 & \dots \\ \dots & 0 & 0 & M_w^{n+1} & \dots \\ & \vdots & \vdots & \vdots & \end{bmatrix}, \tag{10}$$

where

$$M_w^i = \begin{bmatrix} \cos(k_i L) & jz_0 \sin(k_i L) \\ \frac{j}{z_0}\sin(k_i L) & \cos(k_i L) \end{bmatrix}, \quad (i = \dots, n-1, n, n+1, \dots). \tag{11}$$

Here $z_0 = \rho_0 c_0$ is the characteristic impedance of air, $k_i = \omega_i / c_0$ is the wave number of the ith order wave, and L is the length of the waveguide.

III. RESULTS AND DISCUSSION

As the transfer matrix of each component in the system has been developed, we can calculate the transmission and reflection coefficients of arbitrary harmonic modes by converting the transfer matrix into scattering matrix [30]. The parameters in our system are given as $\rho_0 = 1.21$ kg/m^3, $c_0 = 343$ m/s, $\rho_m = 1300$ kg/m^3, $E_m = 117.5$ kPa, $G_m = 40$ kPa, $R = 7.5$ mm, $d = 0.2$ mm. First, we consider a specific case where $T_0 = 2.5$ MPa $\times\, d$ and $m = 0.1$. In this case, the resonant frequency of the membrane without modulation is around 2239 Hz and we choose $f_0 = 2260$ Hz to be the incident frequency. Here the design parameters are modulation frequency $f_m = \frac{\Omega}{2\pi}$ and phase difference $\Delta\phi = \phi_2 - \phi_1$. The evaluation criterion is the transmission coefficient of the fundamental model in the positive direction (t_0^+), while controlling the acoustic wave propagating in the negative direction unamplified or attenuated ($t_n^- \leqslant 1.0$).

By sweeping the modulation frequency and phase difference, we find that the optimal parameters are $f_m = 4450$ Hz and $\Delta\phi = 0.5\pi$ (see the Supplemental Material [36]). Applying the optimized modulation parameters to the system, we can calculate the transmission coefficients of the non-negligible modes as shown in Fig. 2(a). In the positive direction, the pressure amplitude of fundamental mode (0th, 2260 Hz) is amplified 3.0 times, while a non-negligible byproduct (−1st, 2190 Hz) is generated with an amplitude of 2.4. In the negative direction, the amplitude of the 0th and −1st order are 1.0 and 0.5, respectively. There is no surprise in the generation and amplification of the −1st mode in the positive direction as it has also been predicted and verified in the previously reported parametric amplification devices [3,28,30]. Time-dependent transient simulation in Comsol is conducted to verify the theoretical calculation. In the simulation, a monochromatic plane wave is incident from one end of the tube and a transmitted wave is recorded at the other end. The received signal is analyzed using Fourier transform to obtain the amplitude of each frequency component. Good agreement between theory and simulation is observed in Fig. 2(a), and the small deviation can be attributed to the accumulated numerical error in the time-domain simulation. We then analyze the relation between the amplification factor and the modulation depth. As depicted in Fig. 2(b), the amplification factor increases as the modulation depth increases. However, the actual amplification factor that can be achieved is constrained by the weak modulation condition, which suggests that the theoretical model is considered to be accurate when $m \leqslant 0.1$. This means we can get any amplification factor below the threshold by controlling the modulation depth. The threshold denotes the maximum amplification factor under the weak modulation assumption.

In addition to the amplification factor, we have also studied the effective working band of the amplifier. Note that each input frequency in this effective working band has its own modulation parameters for the optimized amplification factor. For time-modulated membranes, it is known that the effective modulation band is typically around its resonant frequency. In this case, the resonant frequency for the unmodulated membrane with a static surface tension $T_0 = 2.5$ MPa $\times\, d$ is 2239 Hz, and the transmission spectrum of this membrane is depicted in Fig. 2(c). The input frequency is swept from 2150 to 2350 Hz with a frequency step of 10 Hz, and all the other parameters are kept unchanged. For each input frequency, we follow the same procedure as mentioned above to find the best modulation parameters combination f_m and $\Delta\phi$. Here an input frequency is defined to be effective if a set of parameters can be found to satisfy both of the following criteria: First, the amplification factor for the positive direction is larger than 2.8. Second, the acoustic wave propagating along the negative

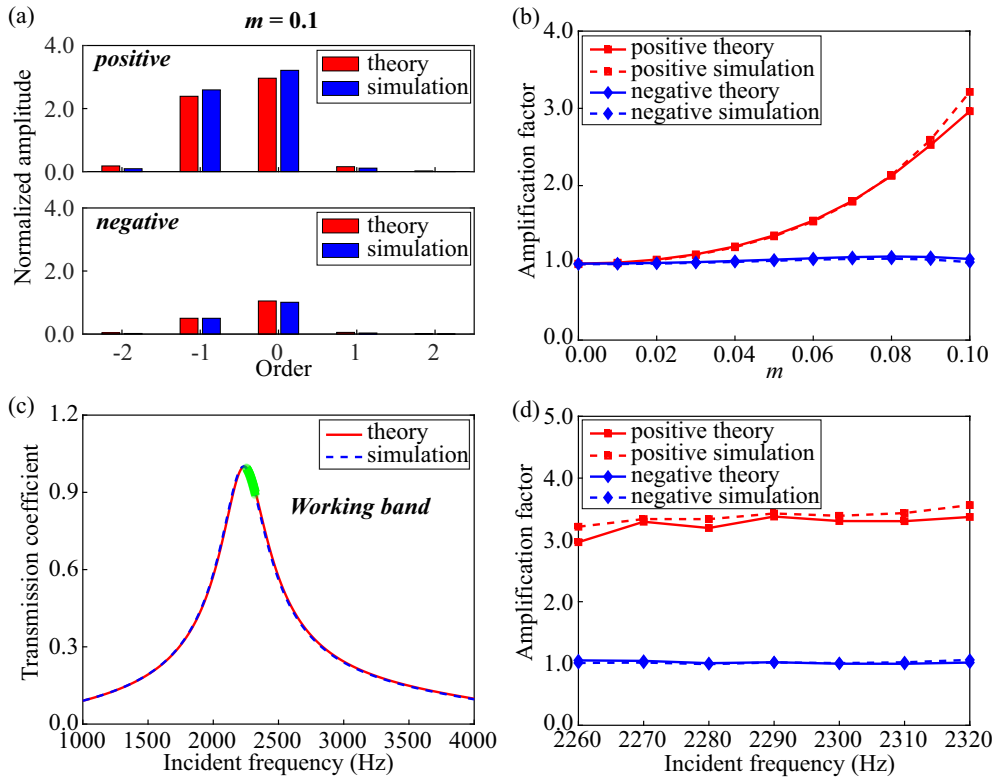

FIG. 2. (a) Amplitude of each frequency component of the modulated transmitted waves under a monochromatic incidence $f_0 = 2260$ Hz, $p_a = 1$. The modulation depth, frequency, and phase difference are 0.1, 4450 Hz, and 0.5π, respectively. Red bars: Results from transfer matrix method in frequency domain; blue bars: results from Comsol simulation in time domain. (b) Amplification factor of the fundamental mode under different modulation depth. Red/blue solid line: Theoretically calculated forward/backward amplification factor; red/blue dashed line: forward/backward simulation results from Comsol. (c) Transmission spectrum of a membrane under a static tension $T_0 = 2.5$ MPa $\times\, d$. Red solid line: Transmission coefficient from theoretical calculation; blue dashed line: transmission coefficient from frequency domain simulation. The effective working frequency range are highlighted. (d) The amplification factor in the working band under this specific surface tension. The modulation depth is 0.1 and each input frequency has its own optimal modulation parameters (modulation frequency and phase difference) for the maximum amplification. Red/blue solid line: Theoretically calculated forward/backward amplification factor; red/blue dashed line: forward/backward simulation results from Comsol.

direction is unamplified ($t_n^- \leqslant 1.0$). From the parametric sweep, we find that the effective working band for the given static tension is 2260–2320 Hz, which is slightly higher than the resonant frequency of the unmodulated membrane as marked in green highlight in Fig. 2(c). The optimized modulation parameters are given in Table I. A series of simulations were carried out with different excitation frequencies and corresponding modulation parameters, and the response of the system was analyzed using Fourier transform. The results are summarized in Fig. 2(d). Good agreement can be observed between transfer matrix calculation and Comsol simulation.

Finally, as we have shown that the effective working band of this structure is always around its resonant frequency, we further study the amplification performance in relation to the resonant frequency of the membrane. Since the resonant frequency is mostly dependent on the static surface tension, it is convenient to adjust the static surface tension T_0 without any change of the geometric configuration. A practical implementation of this adjustment is through an extra DC voltage applied on the membrane, which can be used to control the static tension shift. A series of calculation and simulation are performed to prove this idea. First, we choose five more different static surface tensions, i.e., $T_0 = 2.6$ MPa $\times\, d$, $T_0 = 2.7$ MPa $\times\, d$, $T_0 = 2.8$ MPa $\times\, d$, $T_0 = 2.9$ MPa $\times\, d$, and $T_0 = 3.0$ MPa $\times\, d$. The resonant frequencies of unmodulated membranes under these surface tensions are obtained from the transmission spectrum, which are 2281, 2324, 2367, 2409, and 2450 Hz, respectively. Then, for each surface tension T_0, we sweep the input frequency range around the corresponding resonant frequency and identify the effective amplification band. The working procedures are the same as above and not expanded here for brevity. Finally, all of these five individual working bands together with the one under $T_0 = 2.5$ MPa $\times\, d$ are bridged to construct an integral efficient work band as depicted in Fig. 3. The modulation parameters for each input frequency are provided in Table I. It should be clarified that for two adjacent T_0, the working bands are partially overlapping. We just choose either of them for clearer representation, and the overlapping part are not depicted in Fig. 3. From the figure we can see that as the surface tension T_0 increases, the amplification factor increases gradually. This effect can be explained by the relation between quality factor Q and surface tension T_0. For the same membrane, the larger the surface tension, the higher the quality factor will be. Analysis in a

TABLE I. Modulation parameters for each input frequency.

T_0	f_0 (Hz)	f_m (Hz)	$\Delta\phi$ (rad)
2.5 MPa × d	2260	4450	0.50π
	2270	4470	0.46π
	2280	4480	0.44π
	2290	4500	0.40π
	2300	4510	0.40π
	2310	4520	0.40π
	2320	4530	0.40π
2.6 MPa × d	2330	4590	0.42π
	2340	4600	0.36π
	2350	4610	0.36π
	2360	4620	0.38π
2.7 MPa × d	2370	4670	0.40π
	2380	4680	0.38π
	2390	4700	0.36π
	2400	4710	0.36π
2.8 MPa × d	2410	4750	0.38π
	2420	4770	0.38π
	2430	4780	0.34π
	2440	4790	0.36π
2.9 MPa × d	2450	4830	0.40π
	2460	4850	0.36π
	2470	4860	0.34π
	2480	4870	0.36π
3.0 MPa × d	2490	4910	0.40π
	2500	4930	0.34π
	2510	4940	0.34π
	2520	4950	0.36π

previous work [27] suggests that a higher quality factor can be helpful in the frequency conversion and amplification.

IV. CONCLUSION

To conclude, a tunable unidirectional acoustic amplifier design based on a space-time modulated membrane system is proposed and analyzed theoretically and numerically. As the membranes can be considered as serial loads in the waveguide, the transfer matrix method for a one-dimensional system with space-time modulated loads is applied to analyze this membrane system. By carefully choosing the modulation parameters f_m and $\Delta\phi$, a frequency range slightly above the resonant frequency of an unmodulated membrane is found, in which unidirectional amplification can be realized. As the resonant frequency of a given membrane depends mostly on the static surface tension, a tunable efficient working band (2260–2520 Hz) is constructed by adjusting the static surface tension from 2.5 MPa × d to 3.0 MPa × d. In this effective working band, the positive amplification factor increases gradually from 3.0 to 5.8, while the negative transmission coefficient remains around 1 which means no amplification in the negative direction. The increase of the amplification factor can be attributed to the improvement of the quality factor of the system as the surface tension increases. In this work, the amplifier is only studied in a two-membrane setup. Some constraints are also added to simplify the system, such as identical static surface tension T_0 and same sinusoidal modulation function. Removing these constraints and introducing more design parameters into the system will, in principle, give rise to enhanced amplification performance and many other interesting phenomena. It is believed that by adopting different modulation profiles, this space-time modulated membrane system will have a promising prospect as a feasible implementation for novel functionalities in a number of applications, such as sensing, imaging, and communications.

ACKNOWLEDGMENTS

J.L., C.S., and S.A.C. wish to thank a Multidisciplinary University Research Initiative grant from the Office of Naval Research (Grant No. N00014-13-1-0631) and an Emerging Frontiers in Research and Innovation grant from the National Science Foundation (Grant No. 1641084). X.Z., G.Z., and L.L. wish to thank the National Natural Science Foundation of China (No. 51975142), the Natural Science Foundation of Heilongjiang Province (No. E2017036), and the Assisted Project by Heilongjiang Postdoctoral Funds for Scientific Research Initiation. X.Z. wishes to acknowledge the China Scholarship Council (CSC) for financial support.

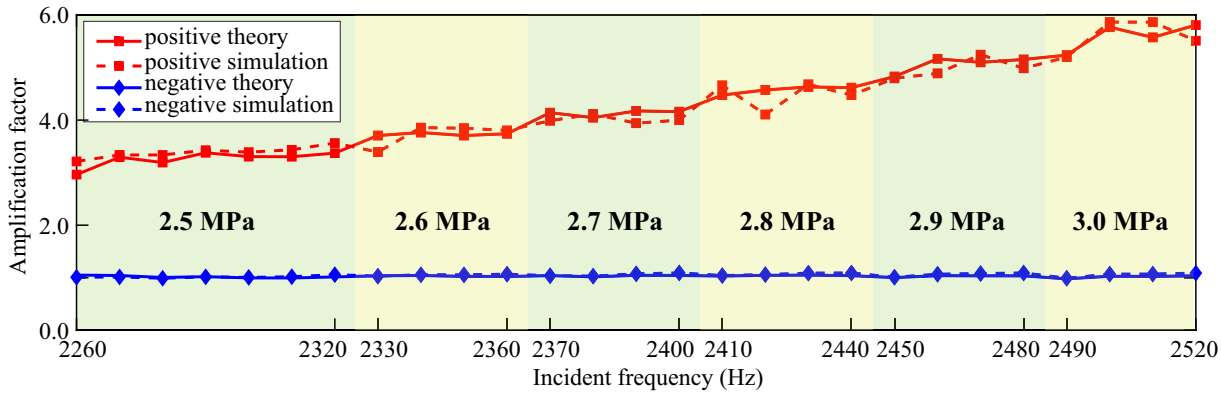

FIG. 3. The effective working frequency range under a static surface tension from $T_0 = 2.5$ MPa × d to $T_0 = 3.0$ MPa × d. The modulation depth keeps 0.1 while the modulation parameters (modulation frequency and phase difference) are well designed for each input frequency. Red/blue solid line: Theoretically calculated forward/backward amplification factor; red/blue dashed line: forward/backward simulation results obtained from Comsol.

[1] P. Tien and H. Suhl, A traveling-wave ferromagnetic amplifier, Proc. IRE **46**, 700 (1958).

[2] P. Tien, Parametric amplification and frequency mixing in propagating circuits, J. Appl. Phys. **29**, 1347 (1958).

[3] A. Cullen, A travelling-wave parametric amplifier, Nature (London) **181**, 332 (1958).

[4] A. Cullen, Theory of the travelling-wave parametric amplifier, Proc. IEE Part B **107**, 101 (1960).

[5] J.-C. Simon, Action of a progressive disturbance on a guided electromagnetic wave, IRE Trans. Microwave Theory Tech. **8**, 18 (1960).

[6] A. Oliner and A. Hessel, Wave propagation in a medium with a progressive sinusoidal disturbance, IRE Trans. Microwave Theory Tech. **9**, 337 (1961).

[7] E. Cassedy and A. Oliner, Dispersion relations in time-space periodic media: Part I Stable interactions, Proc. IEEE **51**, 1342 (1963).

[8] E. Cassedy, Dispersion relations in time-space periodic media: Part II Unstable interactions, Proc. IEEE **55**, 1154 (1967).

[9] Z. Yu and S. Fan, Complete optical isolation created by indirect interband photonic transitions, Nat. Photon. **3**, 91 (2009).

[10] S. Taravati, N. Chamanara, and C. Caloz, Nonreciprocal electromagnetic scattering from a periodically space-time modulated slab and application to a quasisonic isolator, Phys. Rev. B **96**, 165144 (2017).

[11] S. Bhandare, S. K. Ibrahim, D. Sandel, H. Zhang, F. Wust, and R. Noé, Novel nonmagnetic 30-dB traveling-wave single-sideband optical isolator integrated in III/V material, IEEE J. Sel. Top. Quantum Electron. **11**, 417 (2005).

[12] H. Lira, Z. Yu, S. Fan, and M. Lipson, Electrically Driven Nonreciprocity Induced by Interband Photonic Transition on a Silicon Chip, Phys. Rev. Lett. **109**, 033901 (2012).

[13] S. Taravati, Self-biased broadband magnet-free linear isolator based on one-way space-time coherency, Phys. Rev. B **96**, 235150 (2017).

[14] M.-A. Miri, F. Ruesink, E. Verhagen, and A. Alù, Optical Nonreciprocity Based on Optomechanical Coupling, Phys. Rev. Appl. **7**, 064014 (2017).

[15] D. Correas-Serrano, J. Gomez-Diaz, D. Sounas, Y. Hadad, A. Alvarez-Melcon, and A. Alù, Nonreciprocal graphene devices and antennas based on spatiotemporal modulation, IEEE Antennas Wireless Propag. Lett. **15**, 1529 (2015).

[16] N. A. Estep, D. L. Sounas, and A. Alù, Magnetless microwave circulators based on spatiotemporally modulated rings of coupled resonators, IEEE Trans. Microwave Theory Tech. **64**, 502 (2016).

[17] N. Reiskarimian, J. Zhou, and H. Krishnaswamy, A CMOS passive LPTV nonmagnetic circulator and its application in a full-duplex receiver, IEEE J. Solid State Circuits **52**, 1358 (2017).

[18] S. Taravati, Aperiodic space-time modulation for pure frequency mixing, Phys. Rev. B **97**, 115131 (2018).

[19] S. Taravati and A. A. Kishk, Dynamic modulation yields one-way beam splitting, Phys. Rev. B **99**, 075101 (2019).

[20] A. Shaltout, A. Kildishev, and V. Shalaev, Time-varying metasurfaces and Lorentz non-reciprocity, Opt. Mater. Express **5**, 2459 (2015).

[21] Y. Hadad, D. L. Sounas, and A. Alu, Space-time gradient metasurfaces, Phys. Rev. B **92**, 100304(R) (2015).

[22] S. Taravati and C. Caloz, Mixer-duplexer-antenna leaky-wave system based on periodic space-time modulation, IEEE Trans. Antennas Propag. **65**, 442 (2016).

[23] Y. Hadad, J. C. Soric, and A. Alu, Breaking temporal symmetries for emission and absorption, Proc. Natl. Acad. Sci. **113**, 3471 (2016).

[24] D. Ramaccia, D. L. Sounas, A. Alù, F. Bilotti, and A. Toscano, Nonreciprocity in antenna radiation induced by space-time varying metamaterial cloaks, IEEE Antennas Wireless Propag. Lett. **17**, 1968 (2018).

[25] R. Fleury, D. L. Sounas, and A. Alù, Subwavelength ultrasonic circulator based on spatiotemporal modulation, Phys. Rev. B **91**, 174306 (2015).

[26] R. Fleury, A. B. Khanikaev, and A. Alu, Floquet topological insulators for sound, Nat. Commun. **7**, 11744 (2016).

[27] C. Shen, J. Li, Z. Jia, Y. Xie, and S. A. Cummer, Nonreciprocal acoustic transmission in cascaded resonators via spatiotemporal modulation, Phys. Rev. B **99**, 134306 (2019).

[28] J. Li, C. Shen, X. Zhu, Y. Xie, and S. A. Cummer, Nonreciprocal sound propagation in space-time modulated media, Phys. Rev. B **99**, 144311 (2019).

[29] C. Shen, X. Zhu, J. Li, and S. A. Cummer, Nonreciprocal acoustic transmission in space-time modulated coupled resonators, Phys. Rev. B **100**, 054302 (2019).

[30] J. Li, X. Zhu, C. Shen, X. Peng, and S. A. Cummer, Transfer matrix method for the analysis of space-time modulated media and systems, Phys. Rev. B **100**, 144311 (2019).

[31] H. Esfahlani, M. S. Byrne, M. McDermott, and A. Alù, Acoustic supercoupling in a zero-compressibility waveguide, Research **2019**, 2457870 (2019).

[32] H. Li, M. Rosendo-López, Y. Zhu, X. Fan, D. Torrent, B. Liang, J. Cheng, and J. Christensen, Ultrathin acoustic parity-time symmetric metasurface cloak, Research **2019**, 8345683 (2019).

[33] X. Zhu, J. Li, C. Shen, X. Peng, A. Song, L. Li, and S. A. Cummer, Non-reciprocal acoustic transmission via space-time modulated membranes, Appl. Phys. Lett. **116**, 034101 (2020).

[34] K. Uchino, The development of piezoelectric materials and the new perspective, in *Advanced Piezoelectric Materials* (Elsevier, Amsterdam, 2017), pp. 1–92.

[35] F. Bongard, H. Lissek, and J. R. Mosig, Acoustic transmission line metamaterial with negative/zero/positive refractive index, Phys. Rev. B **82**, 094306 (2010).

[36] See Supplemental Material at http://link.aps.org/supplemental/10.1103/PhysRevB.102.024309 for parameter sweeping and sensitivity of the structure.